AUT Journal of Electrical Engineering

AUT J. Electr. Eng., 56(1) (Special Issue) (2024) 113-124
DOI: 10.22060/eej.2023.22007.5503

Design and Optimization of Permanent Magnet Flux-Switching Generator Arrangement Spoke by Taguchi Method for Direct-Drive Wind Turbines

Pouria Nadri, Mohammad Reza Besmi*

Department of Electrical Engineering, Shahed University, Tehran, Iran

ABSTRACT: Due to the unique structure of Permanent Magnet Flux Switching Generators (PMFSG), which involves the interaction of permanent stator magnets and rotor teeth, the generated cogging torque is higher compared to that of other permanent magnet machines, resulting in torque ripple, vibration, and noise. A well-designed machine structure reduces vibration and noise in PMFSG generators while also improving generator performance, machine power, and efficiency. According to related research, PMFSGs are an efficient and attractive solution for wind turbine generator applications and small-scale applications. The cogging torque in the PMFS generator is critical. In this study, a permanent magnet flux switching generator with a spoke arrangement, a toothed rotor with a single-layer slot, and a permanent magnet inside the stator with less cogging torque and higher output power were constructed. Simulations were carried out using the two-dimensional Finite Element Method (FEM) and optimized using the Taguchi method. The best model design will lower effective cogging torque and ripple cogging torque. Finally, the effectiveness of the proposed optimization approach was validated by comparing it to the base model. As a result, the suggested optimization method can be used to effectively design PMFS machines and other types of PM machines used in renewable applications.

Review History:

Received: Dec. 11, 2022
Revised: Jun. 10, 2023
Accepted: Aug. 05, 2023
Available Online: Feb. 01, 2024

Keywords:

Cogging Torque
Finite Element Method
Taguchi Method
Permanent Magnet Flux Switching Generator
Wind Turbine

1- Introduction

Flux-switching machines have evolved as a more appealing sort of machine in recent years than standard electric machines. Direct Current (DC) devices have several disadvantages, including heavy maintenance, low efficiency, limited reliability, and huge size. High efficiency, a high power factor, a high torque/volume ratio, and high torque are significant restrictions that the electric vehicle must overcome for hybrid electric vehicle applications or electric automobiles. The advantages of flux-switching permanent magnet machines include increased rotor strength, reduced cogging torque, high-density torque production, and increased efficiency. These machines are well-suited for applications and operation in severe environments, such as wind turbines, where strength is critical [1-4]. Many academics have recently considered flux-switching permanent magnet machines to be one of electric machines. Flux Switching (FE) machines are a suitable choice for wind farm applications due to their high power, high efficiency, good resistance to demagnetization, simple and sturdy rotor, and good maintainability [5]. One of the basic problems with traditional optimization approaches is that they do not account for design factors and the lengthy time necessary for optimization. To improve the efficiency, performance, and quality of the generator, a precise optimization model should be used to replace the old ones. As a result, a robust optimization strategy is required to improve machine dependability and performance [6]. Various strategies for reducing torque ripple and increasing the output power of flux-switching generators have been presented in recent years. The paper [7] investigates a new partitioned FSPM machine with flux barriers, which boosts flux modulation and Permanent Magnet (PM) utilization by 46.53%. Furthermore, the suggested flux-switching permanent magnet machine rotor pole pair combinations reduce stator flux leakage. This will disable the slot effects. Additionally, partial saturation is decreased, resulting in less cogging torque and torque ripple. The investigation of various topologies of the Double Stator Hybrid Excitation Flux Switching Series (DSHEFSS) and parallel machines has revealed that the double stator hybrid excitation flux switching machines are capable of producing high torque and power when compared to other double stator machine designs [8,9].

*Corresponding author's email: besmi@shahed.ac.ir

Table 1. characteristic of the design parameters

Symbol	Parameters	Symbol	Parameters
M_t	Thickness magnet	Q	Number of stator slot
M_w	Magnet width	P	Number of rotor poles
L_{tooth}	Rotor tooth length	I_{rms}	RMS current
$A_{s\_opening}$	Stator slot opening	δ	Current density
Y_r	Yoke rotor	L	Length of machine
Y_s	Yoke stator	Angle rotor	Rotor slot angle
Ff	Fill factor	R_{s_out}	Outer radius of the stator
R	Resistance	R_{s_in}	Inner radius of the stator
L_g	Length air gap	A_s	Stator slot length

2- Materials and Methods

Electric machine design is a time-consuming process that demands several considerations. There is no standard approach for designing electric machines, and the process varies depending on the type of machine. However there are some standard actions to take in the design process that will be explained further below. The type of machine, its topology, materials, and dimensions utilized during design are determined and matched to the demands and requirements of a certain application in the initial step. The performance parameters of the machine in permanent mode, such as efficiency, torque, torque ripple, output power, materials and manufacturing costs, volume, and so on, are among the requirements. The machine's performance is then evaluated using indicators such as power output, torque, efficiency, and pricing. In the third stage, optimization models are constructed based on the practical plans collected. Optimization objectives, constraints, and parameters must be defined in the optimization model for each design.

2- 1- Taguchi experiment design method

The FEM, which is the most precise method for modeling electric devices, is used to model and assess the proposed generator [10]. The structure of the flux-switching permanent magnet generator with spoke arrangement can be studied and analyzed using FEM, taking into consideration geometric details and nonlinear magnetic properties. As a result, this strategy allows for great accuracy while avoiding several assumptions. The Taguchi experiment design method and the standard table of presentations are utilized for optimization. Finally, the finite element approach is used to compare the results of the initial and optimal designs. To shorten the optimization period, the performance characteristics of the developed machine are optimized utilizing the Taguchi experiment design optimization approach. All simulations are carried out using the Taguchi method and the FEM approach. Taguchi methods are used to compare the outcomes of the original and optimal designs. The acquired results suggest that the Taguchi approach improves the machine's performance characteristics in a short computation period. Taguchi optimization has the advantage of lowering the number of experiments, the cost, and the time required to obtain the optimal point. Furthermore, Taguchi optimization allows for the examination of numerous parameters, such as the kind of consumables, anticipating outcomes in optimal settings, simultaneous optimization for many answers, and the examination of factors with varied levels. The design of the tests is carried out after the basic information has been prepared.

The number of tests required and how to mix the levels of factors in each experiment are established at this step based on the number of factors and the values of the levels of distinct factors. Finally, the experiment design is divided into four steps [11].

2- 2- Analysis of Taguchi

The outcomes of the trials are analyzed in this step, to determine the best settings and calculate the effect of factors on the aim function. If the external arrays are not taken into account in the matrix design and analysis of variance, the mean analysis is applied to the test findings. By examining the mean effects of each level of design factors, mean analysis is used to determine the ideal settings for each design factor. A statistical approach used to determine the effect of each component on the response is the analysis of variance.

The ideal design performance will be predictable once the optimal level for each parameter is identified [12]. The first stage in the study of means is to compute the mean value of the test results (answers), which is acquired from (1).

$$m = \frac{\sum_{j=1}^{k} m_j}{k} \quad (1)$$

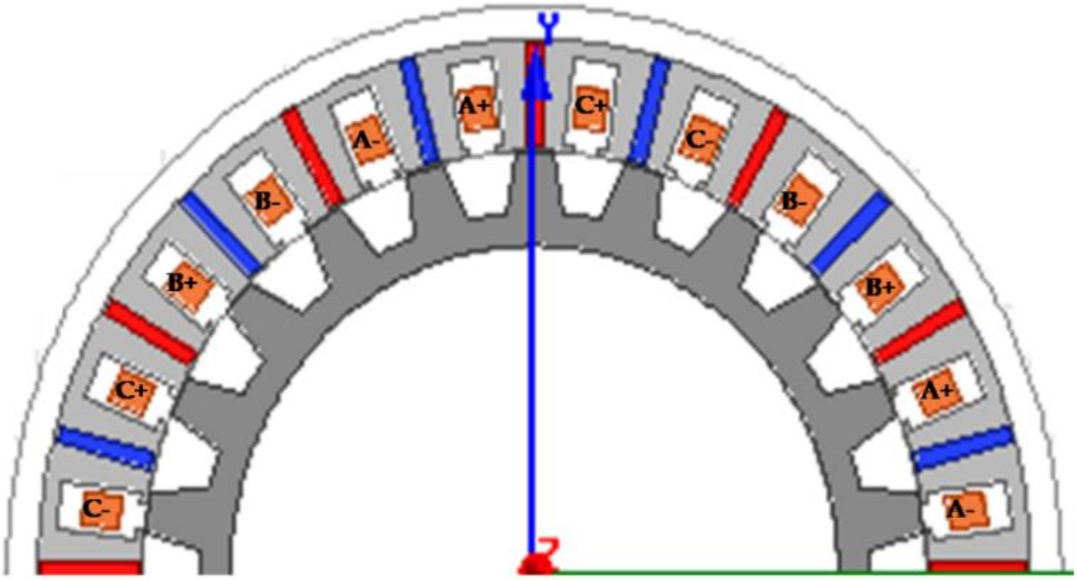

Fig. 1. Prototype generator topology and windings

Where m is the average of the overall test results in the column in question. The number of tests is K, and the average of the test results in the j test of a given column is m_j. If a response is evaluated, the best composition is derived based on the components' average influence and the type of quality feature. An analysis of variance should be performed to identify the ideal values if the purpose is to optimize two or more replies.

The goal of analysis of variance is to identify how changes in all factors affect the overall scatter of responses [12]. The first step in analyzing variance is to get the sum of the squares of each of the factors. The obtained values represent the deviation of the simulation results from the mean value [13]. (2) is used to calculate the sum of the squares of factor A.

$$S_A = \frac{\sum_{j=1}^{k}(m_{A(j)} - m)^2}{Q} \quad (2)$$

In which case, S_A The aim function's variance is under factor A, $m_{A(j)}$ is an average of a given goal function under the j level of factor A, and Q is the number of levels of each factor. The sum of the squares of the other elements is computed similarly [13].

2- 3- Combining Taguchi and Finite Element (FE) Methods for Optimal Design of Permanent Magnetic Flux Switching (PMFS) Generator

The methods for determining electromagnetic torque are divided into two categories: analytical and numerical approaches. The Finite Element Method (FEM) can determine the electromagnetic torque of a machine while accounting for the motor's geometrical complexity as well as magnetic saturation. Analytical techniques continue to be beneficial for predicting electromagnetic torque. The analytical model of the electromagnetic torque employs the Maxwell stress tensor and the virtual work principle.

The electromagnetic torque can be estimated using the radial and tangential flux densities and the Maxwell stress tensor [14]. Taguchi is applied according to the initial design and by modeling the flux-switching permanent magnet generator with FEM to get the output of the machine's experimental design processes. The topology of a flux-switching permanent magnet generator with spoke arrangement, winding, and demarcation is depicted in Fig. 1. According to the findings, stepwise optimization can have a positive impact on individual optimization targets [15].

2- 4- Base model design parameters

Table 1 shows the machine's nominal characteristics and dimensions based on the first design [5]. Changes in machine settings for simulation will be made and implemented based on the composition of matrix arrays to optimally design the machine utilizing the finite element method and the Taguchi experimental design approach.

In this article, optimization with the goals of increasing effective voltage and decreasing effective cogging torque has been chosen as an index for measuring torque fluctuations in the no-load state, which can reduce cogging torque ripple and total harmonic distortion. The parameters of the designed generator are shown in Fig. 2.

The specifications and parameters of the base design generator are shown in Table 2.

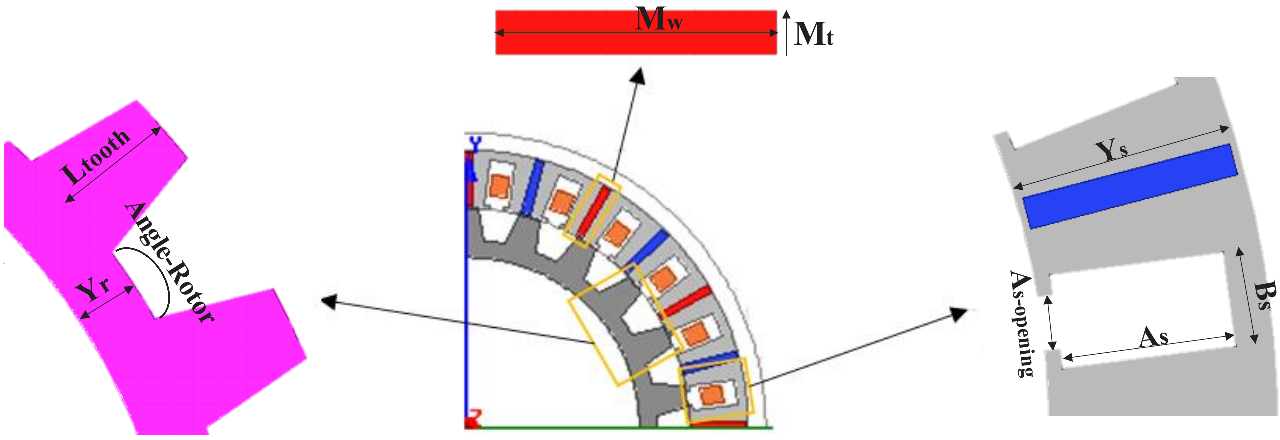

Fig. 2. Designed generator parameters

Table 2. Specifications and parameters of the base design generator

Explanation	parameters	symbol	Quantities / types of materials	unit
Generator structure	Number of stator slot	Q	24	
	Number of rotor poles	P	22	
	Magnet used	Magnet	NdFe35_Spoke	
	RMS current	I_{rms}	١,٦٦٧	A
	Current density	δ	6	A/mm^2
	length of machine	L	100	mm
	Resistance	R	18	ohm
	Rated power	P_{in}	1162.33	W
	Losses	P_{loss}	63.93	W
	RMS cogging torque	$T_{cog\ rms}$	1.36	Nm
Coil specifications	Winding type		Distributed reluctance / single layer	
	Number of windings per phase		٤	
	Number of turns per coil	N_c	١٦٦	
	Fill factor	Ff	0.5	
Specifications of rotor, stator and magnet	Rotor slot angle	Angle_rotor	0.35	degree
	Outer radius of the stator	R_{s_out}	70	mm
	Inner radius of the stator	R_{s_in}	63.3	mm
	Stator slot length	A_s	7.15	mm
	Length air gap	L_g	٠,٣٥	mm
	Thickness magnet	M_t	٢,٤١	mm
	Magnet width	M_w	١٥,٧	mm
	Rotor tooth length	L_{tooth}	٩	mm
	Stator slot opening	$A_{s\_opening}$	٤,٢	mm
	Yoke Rotor	Y_r	٥	mm
	Yoke Stator	Y_s	١٦,٧	mm
	Stator slot width	B_s	١٢,٩	mm

Table 3. Initial values of design variables and test results

Model	Y_r	L_{tooth}	Angle Rotor	$A_{s\ opening}$	V_{rms}	$T_{cog\ rms}$	P_{loss}	P_{out}	η
Base	5 mm	9 mm	0.35 degree	4.2 mm	219.64 v	1.36 Nm	63.93	1098.4 w	94.4%

Table 4. Design parameter symbols in Taguchi trials

Parameter	Y_r	L_{tooth}	Angle Rotor	$A_{s\ opening}$
Symbol	A	B	C	D

2- 5- Design results of the initial FSPM generator

Cogging torque exists in every electromagnetic system that has a stator and a rotating rotor. Because a magnetic circuit's magnetic resistance varies as a function of rotor angle, there is a torque that resists the displacement as the rotor moves from its original low magnetic resistance to a high magnetic resistance. The torque tends to attract the rotor to the next point with the lowest magnetic resistance when it passes through the point with the highest magnetic resistance. This results in an alternating torque waveform known as the cogging torque. The following (3) are used to compute the effective value of the cogging torque:

$$T_{cogging\ RMS} = \sqrt{(\sum_{i=0}^{n}(X_i)^2)/n} \tag{3}$$

Where X_i denotes the amount of gear torque at each point and n denotes the number of points for a period of rotation for the machine under consideration with a rotation speed of 332 rpm equal to 8.2 ms.

(4) can also be used to compute the effective output power:

$$P_{out} = 3.V_{rms}.I_{rms} \tag{4}$$

In each step, V_{rms} is the effective phase voltage per 166 rpm for each coil.

The RMS current value is calculated as follows:

$$Ac = As \times Bs \times Ff \times \delta \tag{5}$$

A_c is the cross section of the conductor, δ is the current density, and S_c is the sum of the conductor surface in (5) parameters.

RMS current calculation in (6):

$$I_{rms} = (As \times Bs \times Ff \times \delta)/Nc \tag{6}$$

In (7), efficiency is calculated.

$$\eta = \frac{P_{out}}{P_{in}} \times 100 \tag{7}$$

Table 3 displays the base values of the design variables as well as the RMS values of the voltage and cogging torque.

2- 6- Optimization of a PMFS generator with spoke arrangement based on modifying the generator's dimensional parameters

Taguchi optimization is a systematic approach to generator design that allows appropriate design optimization decisions to be made to achieve the best results in terms of improving cogging torque, reducing Total Harmonic Distortion (THD), and increasing RMS voltage while taking all design requirements into account. By taking into account the noise factor, design variables, and surface values, this strategy reduces the number of tests and minimizes the effect of uncontrollable factors. The technique of developing Taguchi trials for this machine is explained in the following section, and the results are examined using the finite element approach.

2- 7- Determining test objectives and selecting design parameters

As previously stated, the initial step in Taguchi optimization is to establish optimization targets. Because of the requirements for using a flux-switching permanent magnet spoke generator, the ability to improve the effective cogging torque, increase the effective voltage, and reduce overall harmonic distortion is regarded as an optimization target. Fig. 3 shows the parametric model of the variables intended for optimization. For this purpose, four parameters will be selected under the following headings. Fig. 3 depicts the parametric model of the variables to be optimized. Four parameters will be chosen for this purpose under the following topics:

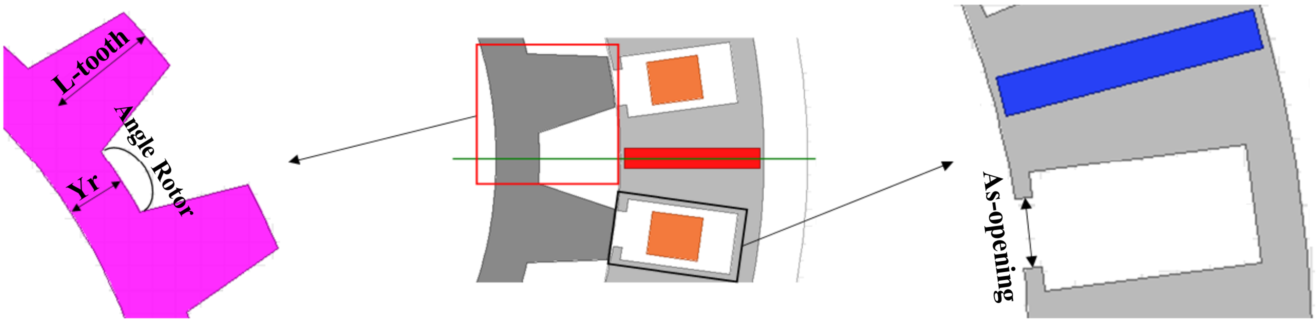

Fig. 3. Taguchi method design variables

Table 5. Design variables and surface values

Level	A (mm)	B (mm)	C (degree)	D (mm)
Level 1	**16**	**5**	**0.32**	**2**
Level 2	**17**	**6**	**0.34**	**2.5**
Level 3	**18**	**7**	**0.36**	**3**
Level 4	**19**	**8**	**0.38**	**3.5**
Level 5	**20**	**9**	**0.4**	**5**

Five effective levels are chosen for each design variable and are shown in Table 5.

To choose the levels listed in Table 5, optimization was performed across a wide variety of dimensions. The basic parameters of the fixed rotor are evaluated in the first stage, and all stator parameters are optimized in a greater numerical range using the Taguchi method before the most effective stator parameters are chosen. The primary stator parameters are deemed fixed in the second stage, and all rotor parameters are optimized in a greater numerical range using the Taguchi method. The most effective rotor parameters have been chosen at this point. In the third stage, the influential parameters determined in the first and second steps for the rotor and stator were positioned adjacent to each other, and the Taguchi method was used to optimize in a wide numerical range once more. The outcomes of the tests were then examined. Following that, there were five levels for each of the four parameters with the greatest influence. Table 5 displays these levels. The third-stage findings demonstrate that selecting levels 1–5 for each parameter produces the greatest outcomes. So, utilizing Table 5 and the Taguchi approach, the major optimization was carried out, and the results are displayed in Table 6 together with Fig. 4. Finally, Table 8 displays the final optimization results.

2- 8- Determination of Taguchi experimental matrix and simulation results

The Taguchi experimental table was generated using the matrix experiment concept based on the optimization parameters of the four variables specified in Fig. 3 and the five-level factor range assigned to each variable. The orthogonal array L25 is analyzed in Table 3 based on the number of variables and levels chosen. Using this strategy, the number of experiments necessary to optimize the design was decreased from a total of $5^4 = 625$ to 25. Reducing the number of tests required to optimize machine performance saves substantial time due to the duration of the solution process in the finite element. Maxwell simulation software was used for all experiments. Table 6 displays the array matrix as well as the outcomes of the relevant tests.

2- 9- Taguchi analysis and selection of the optimal combination of design parameters

To optimize the Taguchi approach, a combination of design parameters will be chosen to provide the least cogging torque and the highest RMS voltage.

2- 9- 1- Minimum cogging torque and Maximum RMS voltage

The design parameters will be chosen based on Fig. 4 to achieve the lowest cogging torque and the highest RMS no load voltage. Based on this, the ideal values of the parameters in Table 4 that result in the lowest cogging torque are $A_{s\text{-}opening} = 2$, $L_{tooth} = 5$, Angle-Rotor = 0.4, and $Y_r = 19$. Furthermore, the ideal values of the parameters that result in the highest RMS voltage at no load are $A_{s\text{-}opening} = 2.5$, $L_{tooth} = 6$, Angle-Rotor = 0.34, and $Y_r = 19$. According to Taguchi's analysis, combining the design parameters of Fig. 4 results in the optimization of cogging torque and RMS voltage.

Table 6. Results of Taguchi optimization experiments

Models	$A_{(mm)}$	$B_{(mm)}$	$D_{(mm)}$	$C_{(deg)}$	$V_{max\ (V)}$	$V_{rms\ (V)}$	$T_{cog\text{-}max\ (Nm)}$	$T_{cog\text{-}min\ (Nm)}$	$T_{cog\text{-}dif\ (Nm)}$	$T_{cog\text{-}rms\ (Nm)}$	$P_{out\ (W)}$
1	16	5	2	0.32	394.69	210.57	3.73	-3.86	7.59	1.66	1053.06
2	16	6	2.5	0.34	417.26	222.90	2.27	-2.71	4.98	1.18	1114.72
3	16	7	3	0.36	410.24	220.85	5.81	-5.85	11.66	2.41	1104.47
4	16	8	3.5	0.38	409.38	218.73	6.4	-6.27	12.67	3.31	1093.87
5	16	9	5	0.4	325.91	198.19	6.18	-4.43	10.61	2.99	991.15
6	17	5	3	0.34	421.78	220.74	4.63	-4.33	8.96	2.27	1103.92
7	17	6	3.5	0.36	431.51	220.62	6.32	-6.84	13.16	2.87	1103.32
8	17	7	5	0.38	350.68	206.58	4.77	-4.5	9.27	1.9	1033.11
9	17	8	2	0.4	422.11	218.4	1.34	-1.26	2.6	0.55	1092.21
10	17	9	2.5	0.32	421.98	220.61	5.79	-5.95	11.74	2.29	1103.27
11	18	5	5	0.36	385.46	210.67	3.32	-3.61	6.93	1.37	1053.56
12	18	6	2	0.38	413.64	220.32	4.52	-4.84	9.36	1.75	1101.82
13	18	7	2.5	0.4	420.72	218.42	1.8	-1.65	3.45	0.96	1092.32
14	18	8	3	0.32	409.03	222.06	4.97	-5.02	9.99	2.23	1110.52
15	18	9	3.5	0.34	449.71	228.60	8.35	-10.32	18.67	4.77	1143.68
16	19	5	2.5	0.38	426.25	220.82	3.18	-2.97	6.15	1.33	1104.32
17	19	6	3	0.4	399.78	214.97	2.12	-3.17	5.29	0.95	1075.06
18	19	7	3.5	0.32	418.07	224.98	9.19	-10.62	19.81	4.13	1125.12
19	19	8	5	0.34	419.6	220.4	2.94	-2.49	5.43	1.41	1102.22
20	19	9	2	0.36	392.05	220.78	4.09	-3.97	8.06	1.82	1104.12
21	20	5	3.5	0.4	387.15	212.13	5.4	-5.14	10.54	2	1060.86
22	20	6	5	0.32	433.36	220.07	4.48	-4.5	8.98	2.07	1100.57
23	20	7	2	0.34	412.26	220.22	3.59	-3.72	7.31	1.61	1101.32
24	20	8	2.5	0.36	401.28	223.2	5.81	-5.57	11.38	2.31	1116.22
25	20	9	3	0.38	421.83	221.01	3.61	-4.25	7.86	1.84	1105.27

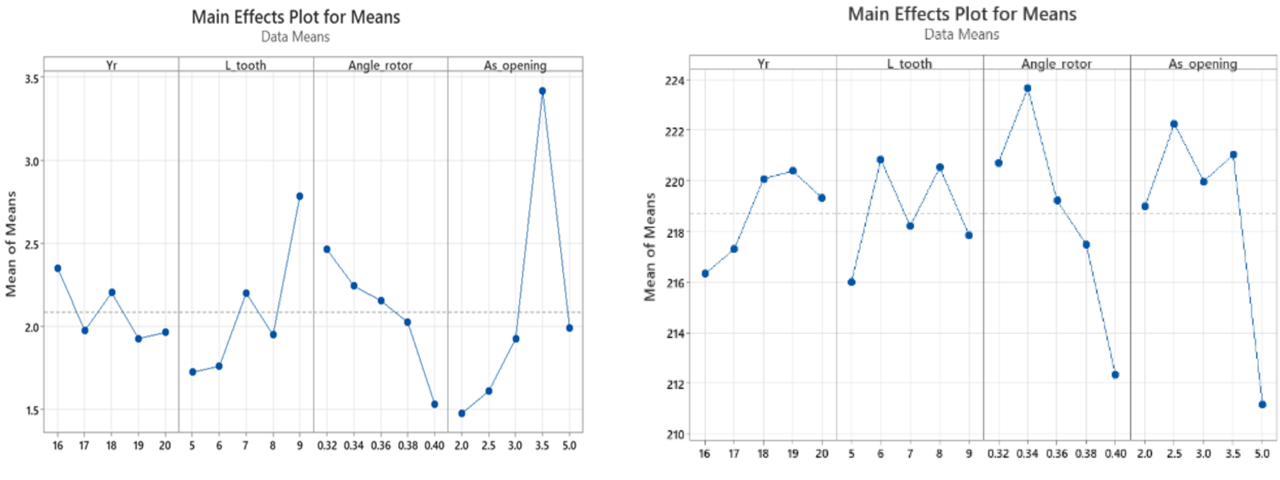

(a) (b)

Fig. 4. Impact of design factor levels on (a) optimal Tcog-rms (Nm) and (b) optimal Vrms (V)

Table 7. Impact of coefficients of optimization parameters

Model	Optimal $T_{cog\text{-}rms}$	Optimal V_{rms}
A	5.8	6.26
B	1.17	5.81
C	1.83	1.33
D	0.33	1.04

Table 8. A comparison between parameters and results of initial and optimal models

	Base	Optimal 1	Optimal 2	Comparision		
Specifications	Initial	Optimal $T_{cog.rms}$	Optimal V_{rms}	Base-optimal 1	Base-optimal 2	Unit
A	5	19	19	*	*	mm
B	9	5	6	*	*	mm
C	0.35	0.4	0.34	*	*	degree
D	4.2	2	2.5	*	*	mm
V_{rms}	219.64	216.91	222.94	-1.24%	1.5%	volt
V_{max}	382.07	417.13	416.9	9.17%	9.11%	volt
$T_{cog\text{-}max}$	3.44	0.4	2.24	88.37%	34.88%	Nm
$T_{cog\text{-}min}$	-2.30	-0.61	-2.7	73.47%	-17.39%	Nm
$T_{cog\text{-}ripple}$	5.74	1.01	4.94	82.4%	13.93%	Nm
$T_{cog\text{-}rms}$	1.36	0.17	1.18	87.5%	13.23%	Nm
P_{out}	1098.41	1084.76	1114.92	-1.24%	1.5%	W
P_{loss}	63.93	64.16	64.58	-0.36%	-1.01%	W
η	94.49	94.41	94.52	-0.08%	0.03%	%

2- 9- 2- Analysis of variance of maximum RMS voltage

Table 7 shows the influence of each parameter's coefficient while optimizing with the purpose of minimizing RMS cogging torque and increasing RMS voltage.

3- Results

In Table 8, the results of the basic model, optimal model 1, and optimal model 2 have been thoroughly compared. The purpose of optimal model 1 is to optimize cogging torque, and the goal of optimal model 2 is to optimize effective voltage. The specifications of the suggested generator are listed in Table 8, including its output power, losses, efficiency, maximum voltage, minimum cogging torque, maximum cogging torque ripple, and effective voltage.

Fig. 5 depicts the construction of the FSPM generator. Fig. 5(a) depicts the structure of the fundamental model. Fig. 5(b) depicts the ideal model's structure, which tries to optimize cogging torque. Another construction of the improved model is presented in Fig. 5(c) to increase the effective voltage.

Fig. 6 depicts the flux density of the best models. The flux density distribution of the FSPM generator has been modeled for wind turbine applications, as can be observed. The contents of the flux density form of two final optimized models are extracted using finite element analysis in Maxwell software. Fig. 6 depicts the relevant FEM simulation after determining the maximum flux density value. As can be seen, the flux density incorporates many spectra and produces optimal results.

Magnetic flux is defined as the number of magnetic field lines passing through a given closed surface and provides a measure of the total magnetic field passing through a given surface. To calculate it, the direction of the magnetic field as well as the half line perpendicular to the surface are needed. If the magnetic field is parallel and aligned with the desired surface, the magnetic flux lines cannot pass through the surface, and if the magnetic field is perpendicular to the surface, the magnetic flux will be at its maximum. Fig. 7 shows the flow lines of the optimized models. As can be seen from the figure, the flux lines have flowed regularly and symmetrically from the rotor teeth towards the stator, which shows the principled and suitable winding for the structure of this generator.

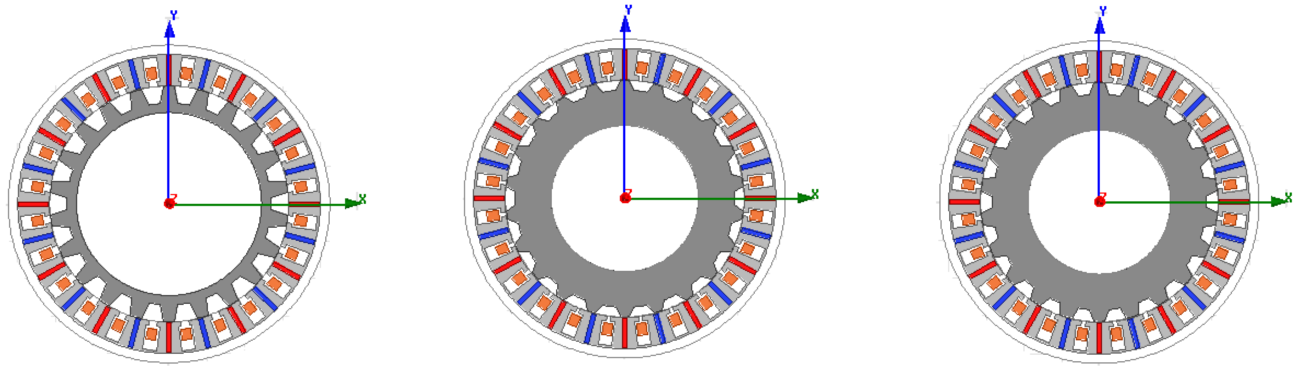

(a) (b) (c)

Fig. 5. Model structure (a) base (b) optimal RMS cogging torque (c) optimal RMS voltage

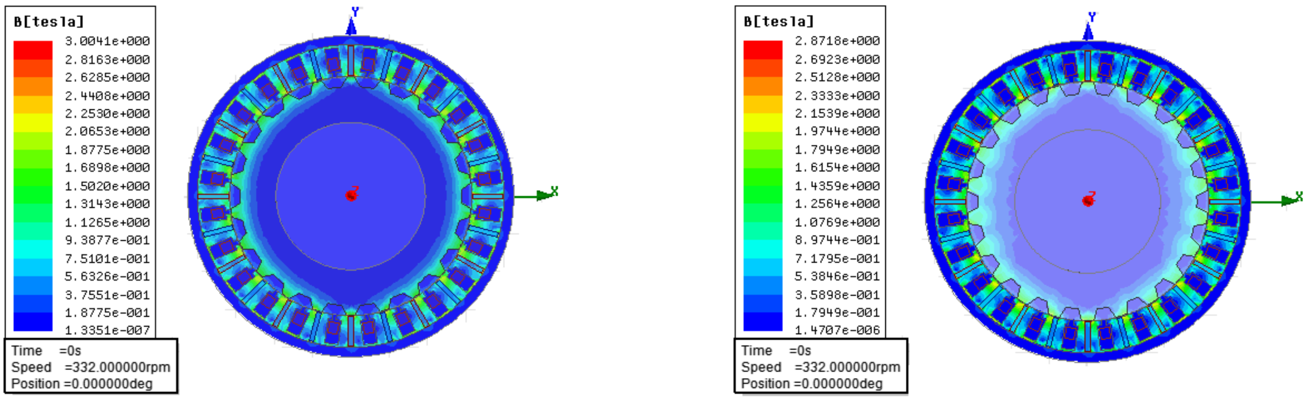

(a) (b)

Fig. 6. Flux density of the model (a) optimal rms cogging torque; (b) optimal rms voltage

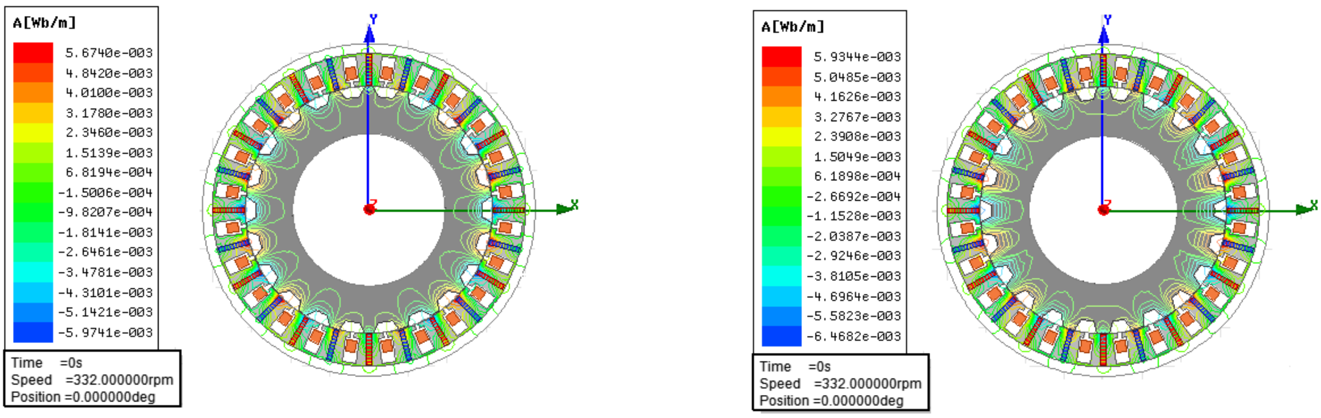

Fig. 7. Flux lines of the model (a) optimal rms cogging torque (b) optimal rms voltage

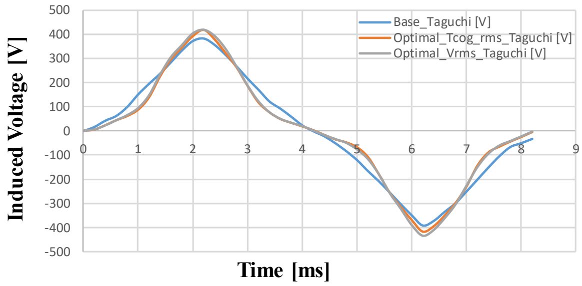

(a)

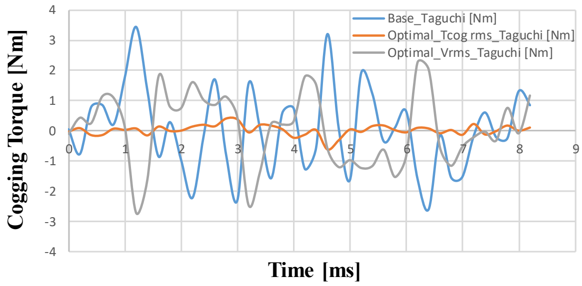

(b)

Fig. 8. Comparison of results-based and optimal models in (a) induced voltage and (b) cogging torque

The induction voltage and cogging torque results for the basic, optimal 1, and ideal 2 models from Table 8 are shown in Fig. 8 throughout a cycle time. In Fig. 8(a), the induced voltage of the initial and ideal models is shown in volts. Fig. 8(b) also shows the cogging torque of the initial and ideal models in Nm. The optimal model's cogging torque ripple has been considerably reduced, as seen in Fig. 8(b).

4- Conclusions

In this article, the Taguchi approach was used to optimize a flux-switching permanent magnet generator. The optimization was performed to first lower the effective cogging torque and its ripple and then optimize the effective voltage. A variety of tests were conducted at various levels for this goal, and the most effective characteristics were chosen for the design of the generator size. The Taguchi optimization approach was then used to reduce cogging torque ripple (Tcog-ripple) by 82.4% in ideal model 1. A small voltage loss follows this significant decrease. In addition, the effective voltage (Vrms) increased by 1.5% in ideal model 2, while the cogging torque ripple (Tcog-ripple) fell by 13.93%. FEM simulation was utilized to validate the suggested optimization, and comparisons were made between the basic model and the proposed optimal models. This comparison demonstrated Taguchi's method's efficiency and effectiveness. The results demonstrate that the optimized models of the proposed FSPM generator have greatly improved.

References

[1] Kumar. A, Srivastava. A, Performance Investigation of Various Flux-Switching Machines for Hybrid Electric Vehicles: A Review, Int. J. of Advanced Res. in Electrical, Electronics and Instrumentation Eng, 5 (2016) 2320-3765.

[2] Somesan. L, Padurariu. E, Viorel. I.A, Szabo. L, Design of a permanent magnet flux-switching machine, IEEE In 2012 ELEKTRO, (2012) 256-259. [CrossRef]

[3] Hua. W, Zhang. G, Cheng. M, Investigation and design of a high-power flux-switching permanent magnet machine for hybrid electric vehicles, IEEE Transactions on magnetics, 51 (2015) 1-5. [CrossRef]

[4] Hua. W, Cheng. M, Zhu. Z. Q, Zhao. W, Kong. X, Comparison of electromagnetic performance of brushless motors having magnets in stator and rotor, Journal of Applied Physics, 103 (2008) 07F124. [CrossRef]

[5] Vladimir. P, Vladimir. D, Vadim. K, Ekaterina. A, Comparison of Flux-Switching and Interior Permanent Magnet Synchronous Generators for Direct-Driven Wind Applications Based on Nelder–Mead Optimal Designing, Mathematics, 9 (2021) 732. [CrossRef]

[6] Vahedi. A, Meo. S, Zohoori. A, An AHP-based approach for design optimization of flux-switching permanent magnet generator for wind turbine applications, International Transactions on Electrical Energy Systems, 26 (2016) 1318–1338. [CrossRef]

[7] Wasiq. U, Faisal. K, Erwan. S, Muhammad. U, Torque characteristics of high torque density partitioned PM consequent pole flux switching machines with flux barriers, CES Trans. Magn., 4 (2020) 130-141. [CrossRef]

[8] Hassan. A, Erwan. S, Roziah. A, Mahyuzie. J, Zarafi. M, Faisal. K, Review of Double Stator Flux switching machines with various arrangements of excitation sources, Alexandria Engineering Journal, 60 (2021) 4393-4410. [CrossRef]

[9] Hao. C, Ayman. E. R, Nabeel A. O. D, Flux-switching permanent magnet machines: a review of opportunities and challenges-part I: fundamentals and topologies, IEEE Trans.Magn, 35 (2020) 684-698. [CrossRef]

[10] Kumar. A, Marwaha. S, Singh. A, Marwaha. A, Performance investigation of a permanent magnet generator, Simulation Modelling Practice and Theory, 17 (2009) 1548-1554. [CrossRef]

[11] Sorgdrager. A. J, Wang. R-J, Grobler. A. J, Taguchi method in electrical machine design, SAIEE African Research Journal, 108 (2017) 150-164. [CrossRef]

[12] Karimpour. S. R, Besmi. M. R, Mirimani. S. M, Multi-objective optimization design and Verification of Interior PMSG Based on Finite Element Analysis and Taguchi method, International Journal of Engineering, 34 (2021) 2097-2106. [CrossRef]

[13] Karimpou. S. R, Besmi. M. R, Mirimani. S. M, Optimal design and verification of interior permanent magnet

synchronous generator based on FEA and Taguchi method, International Transactions on Electrical Energy Systems, 30 (2020) 12597. [CrossRef]

[14] Chen. X, Hu. J, Chen. K, Peng. Z, Modeling of electromagnetic torque considering saturation and magnetic field harmonics in permanent magnet synchronous motor for HEV, Simulation Modelling Practice and Theory, 66 (2016) 212-225. [CrossRef]

[15] Li. F, Zhu. X, Comparative Study of Stepwise Optimization and Global Optimization on a Nine-Phase Flux-Switching PM Generator, Energies, 14 (2021) 4754. [CrossRef]

HOW TO CITE THIS ARTICLE

P. Nadri, M. R. Besmi, Design and Optimization of Permanent Magnet Flux-Switching Generator Arrangement Spoke by Taguchi Method for Direct-Drive Wind Turbines, AUT J Electr Eng., 56(1) (Special Issue) (2024) 113-124.

DOI: 10.22060/eej.2023.22007.5503